EDGE ARTICLE

Check for updates

Synthetic methodology towards allylic *trans*-cyclooctene-ethers enables modification of carbohydrates: bioorthogonal manipulation of the *lac* repressor†

Mark A. R. de Geus, [ID] G. J. Mirjam Groenewold, Elmer Maurits, Can Araman [ID] * and Sander I. van Kasteren [ID] *

The inverse electron-demand Diels–Alder (IEDDA) pyridazine elimination is one of the key bioorthogonal bond-breaking reactions. In this reaction *trans*-cyclooctene (TCO) serves as a tetrazine responsive caging moiety for amines, carboxylic acids and alcohols. One issue to date has been the lack of synthetic methods towards TCO ethers from functionalized (aliphatic) alcohols, thereby restricting bioorthogonal utilization. Two novel reagents were developed to enable controlled formation of *cis*-cyclooctene (CCO) ethers, followed by optimized photochemical isomerization to obtain TCO ethers. The method was exemplified by the controlled bioorthogonal activation of the *lac* operon system in *E. coli* using a TCO-ether-modified carbohydrate inducer.

Introduction

Bioorthogonal bond cleavage reactions have garnered significant interest in recent years.[1–4] Amongst these new "click-to-release" reactions, the inverse electron-demand Diels–Alder (IEDDA) pyridazine elimination has shown particular promise for bioorthogonal utilization.[5] The method employs a *trans*-cyclooctene (TCO) carrying an allylic substituent that upon [4 + 2] cycloaddition with a 1,2,4,5-tetrazine results in the formation of a 4,5-dihydropyridazine.[6] This 4,5-tautomer can rearrange to form two new tautomers of which the 1,4-tautomer can release the allylic payload, followed by rearomatization to the pyridazine (Fig. 1A).[7,8] The excellent biocompatibility and high bimolecular reaction rate of the IEDDA pyridazine elimination[9] has given rise to a multitude of *in vitro* and *in vivo* applications such as the regulation of protein activity[10–12] and the activation of pro-drugs, in which spatiotemporal control is achieved by antibody–drug conjugates (ADCs),[13–15] nanoparticles,[16] enzymatic supramolecular self-assembly[17] or hydrogel injection.[18,19]

To date, nearly all applications for this reaction have relied on the protection of (primary) amines as TCO-carbamates (Fig. 1A, green). Recently, Robillard[8] and Bernardes[20,21] showed that release of other functional groups, such as carboxylic acids (from TCO-esters) and alcohols (from TCO-carbonates or TCO-ethers), is indeed possible (Fig. 1A, orange

and red). Whilst TCO-esters and carbonates suffer from reduced hydrolytic stability in biological systems,[8,20,21] TCO-ethers are particularly appealing due to their high stability and surprisingly fast decaging kinetics when compared to vinyl ether analogues.[8,22–24] Unfortunately, widespread use of TCO-ethers is constricted by their challenging synthesis. Formation of the crucial *cis*-cyclooctene (CCO) ether bond, employing either Mitsunobu chemistry or nucleophilic substitution of a primary alkyl bromide with **1**, is followed by photochemical isomerization[25] to the TCO-ether and isolation of the desired axial isomer (Fig. 1B, top).[8] One exception is the direct alkylation of axial TCO-OH to form a benzylic TCO-ether.[8] Additionally, Bernardes and co-workers developed a self-immolative linker in which a TCO-carbamate is connected to a benzyl ether (Fig. 1B, bottom).[21] Although **1** was used as a Mitsunobu substrate with moderate success,[8] this method essentially limits the scope to phenolic nucleophiles without including the formation of ethers from aliphatic alcohols.[26] Furthermore, direct nucleophilic substitution with **1** is limited to primary positions,[8] in which the desired aliphatic alcohol requires an additional transformation into a leaving group. The self-immolative linker[21] requires at least four synthetic steps from the substrate, which to date has also been limited to phenols. Taken together, synthesis and utilization of TCO-ethers derived from functionalized aliphatic alcohols encountered in biological systems is currently unfeasible. This led us to develop novel synthetic methods for the (regioselective) installation of TCO-ethers in biomolecules as caging moieties, based on reagents **2** and **3**, which we present here (Fig. 1C). Furthermore, we applied our method to enable the synthesis and bioorthogonal

Leiden Institute of Chemistry, The Institute for Chemical Immunology, Leiden University, Einsteinweg 55, 2333 CC Leiden, The Netherlands. E-mail: m.c. araman@lic.leidenuniv.nl; s.i.vankasteren@lic.leidenuniv.nl
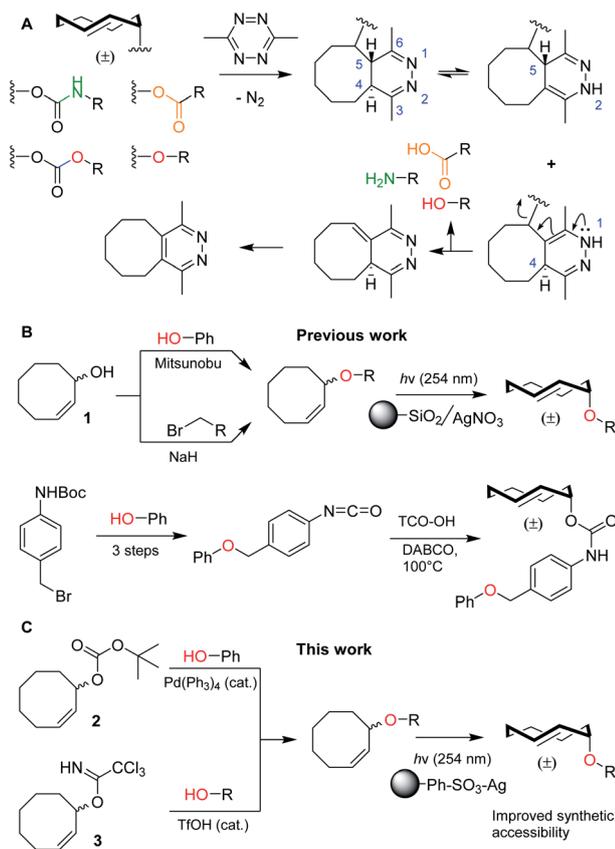
Fig. 1 (A) Overview of the inverse electron-demand Diels–Alder (IEDDA) pyridazine elimination reaction, including the current scope of this method to decage carbamates, carbonates, ethers and esters to obtain amines (green), alcohols (red) and carboxylic acids (orange), respectively. (B) Overview of the current synthetic methods to obtain allylic TCO ethers, including methods from Robillard and co-workers (top)[8] and Bernardes and co-workers (bottom).[21] (C) Novel synthetic methods described in this work, including reagents **2** and **3**.

decaging of a TCO-ether modified carbohydrate, as no TCO-protected variants of these biomolecules currently exist.

Results and discussion

We envisioned a two-step procedure in which the use of electrophilic cyclooctene reagents secured formation of a CCO-ether bond under mild conditions, followed by photochemical isomerization[25] to the desired TCO-ether. Palladium catalysis enables mild, decarboxylative conversion of allyl carbonates to allyl ethers *via* a reactive π-allyl cation species.[27,28] We found a ring strained variant of this reaction was feasible for phenols by transforming *para*-nitrophenyl carbonate **4** into cyclooctene ether **5** under Pd(PPh$_3$)$_4$ catalysis (50 °C) in 92% yield (Scheme 1). Based on this initial observation, we reasoned the palladium-catalyzed method for direct allylation by Grover and co-workers[29] would enable cyclooctene ether formation in a single step. We designed cyclooctene *tert*-butyl carbonate reagent **2**, which decarboxylates upon coordination with a palladium catalyst (Scheme 2A). The spectator *tert*-butoxide formed in this step[29] ensures rapid deprotonation of the phenol nucleophile,
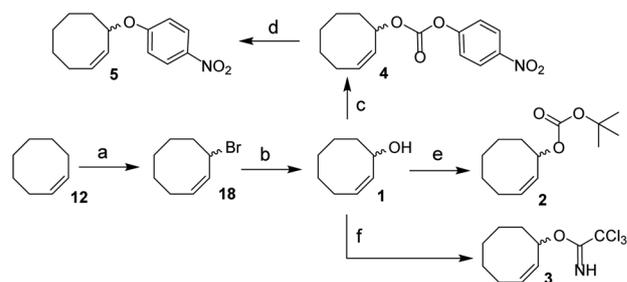
Scheme 1 Synthesis of **1**, **2**, **3**, **4** and **5** from *cis*-cyclooctene (**12**). Reagents/conditions: (a) NBS, AIBN, cyclohexane, reflux, 71%; (b) acetone, H$_2$O, NaHCO$_3$, reflux, 83%; (c) 4-nitrophenyl chloroformate, pyridine, DCM, 0 °C to rt, 83%; (d) Pd(PPh$_3$)$_4$, toluene, 50 °C, 92%; (e) NaHMDS, Boc-ON, THF, 0 °C to rt, 81%; (f) trichloroacetonitrile, DBU, NaHCO$_3$, DCM, 0 °C to rt, ~80% (Table S1†).
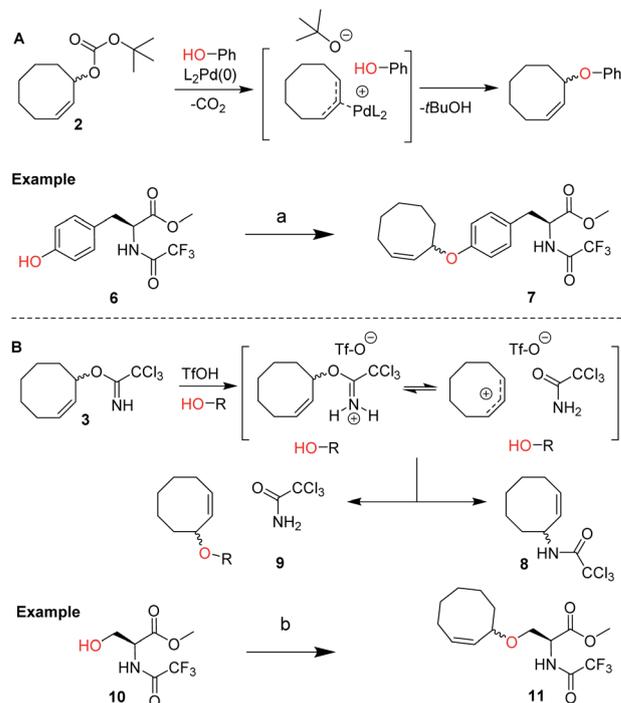
Scheme 2 (A) Design of cyclooctene *tert*-butyl carbonate reagent **2** for the palladium catalyzed installation of cyclooctene ethers on phenols, including the proposed mechanism based on the work of Grover and co-workers.[19] Reagents/conditions: (a) **2**, Pd(PPh$_3$)$_4$, dioxane, 80 °C, 80%; (B) design of cyclooctene trichloroimidate reagent **3** for the Lewis acid triggered formation of cyclooctene ethers from aliphatic alcohols. Proposed mechanism and products observed upon treating **3** with catalytic triflic acid are shown. Reagents/conditions: (b) **3**, TfOH, DCM, −35 °C to 0 °C, 46% (Table S2†).

which can subsequently attack the π-allyl electrophile to form the ether bond. We examined the cyclooctene ether formation with *N*-trifluoroacetyl-protected L-tyrosine methyl ester **6** using reagent **2** (1.2 equivalents) under Pd(PPh$_3$)$_4$ catalysis (80 °C) instead of the previously reported Mitsunobu procedure (12% yield),[8] obtaining cyclooctene ether **7** in 80% yield (Scheme 2A).

In parallel, we designed a second reagent (**3**) for the synthesis of cyclooctene ethers from aliphatic alcohols (Scheme 2B).

Lewis acid triggered activation of cyclooctene trichloroimidate **3** can result in elimination and rearrangement pathways, including the formation of ionic intermediates.[30,31] Cyclooctene trichloroamide **8** (see ESI† for characterization), trichloroacetamide (**9**) and the desired cyclooctene ether can be formed from these reactive intermediates. N-trifluoroacetyl-protected L-serine methyl ester **10** was alkylated using 2 equivalents of **3** under triflic acid catalysis (−35 °C to 0 °C) to obtain **11** in 46% yield (Scheme 2B, Table S2†). Furthermore, reagents **2** and **3** were both synthesized from *cis*-cyclooctene (**12**) in 3 steps (∼48% yield) with a common intermediate (**1**) and a single chromatographic purification (Scheme 1, Table S1†).

Carbohydrates orchestrate a diverse array of biological processes and as such, spatiotemporal control over these biological activities would be a powerful addition to the "click-to-release" toolkit. A classic example of a biological process directed by glycans is the switching of the *lac* operon.[32,33] It is a regulatory element that is used to control nutrient-dependent transcription in *E. coli*. When lactose concentration is low, the activity of the operon is inhibited by a repressor element.[34] When the concentration of lactose increases, it will bind to the repressor, leading to a decreased affinity of the lactose–repressor complex for the operon.[35] This results in enhanced gene transcription for proteins under control of this promotor. This system has been extensively used for the expression of recombinant proteins in *E. coli* and the synthetic *lac* operon inducer isopropyl β-D-1-thiogalactopyranoside (IPTG, **13**) is a key reagent here. Control over its activity has previously been attempted using both photochemical[36] and hypoxia-triggered[37] induction strategies. We therefore deemed it an excellent model carbohydrate to test IEDDA pyridazine elimination on carbohydrates. Initial experiments with peracetylated IPTG (**14**) under conditions typically used for photochemical isomerization of cyclooctenes confirmed the high affinity of the thioacetal functionality towards the silver nitrate used for enrichment of the TCO-isomers upon photoisomerization (Scheme 3). We therefore designed a novel inducer for the *lac* operon, substituting the sulfur with oxygen to obtain an O-glycoside, isopropyl β-D-1-galactopyranoside (IPG, **15**, Scheme 4).

Starting from peracetylated β-D-galactopyranoside **16**, installation of the beta isopropyl group on the anomeric center was achieved in a one-pot, two-step procedure in 70% yield. The 'disarmed' pentaacetate was first transformed into an anomeric
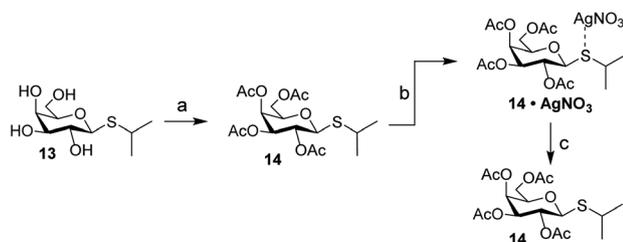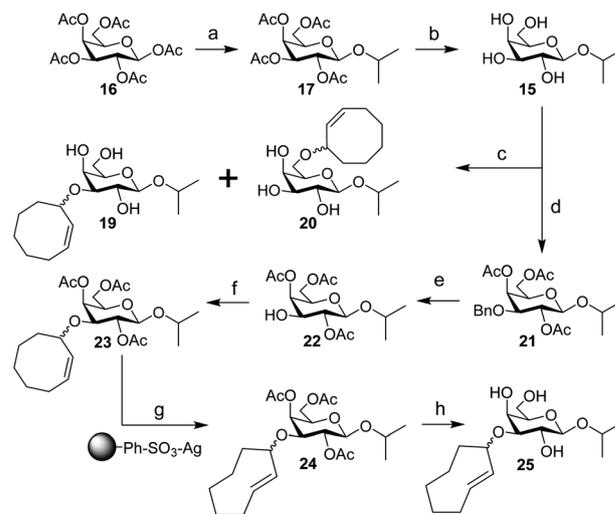
Scheme 4 Synthesis of IPG (**15**), 3-CCO-IPG (**19**), 6-CCO-IPG (**20**), and 3-TCO-IPG (**25**) from peracetylated β-D-galactopyranoside (**16**). Reagents/conditions: (a) (i) HBr, AcOH, DCM, 0 °C to rt; (ii) 2-propanol, I₂, DCM, 0 °C to 4 °C, 70% over 2 steps; (b) NaOMe, MeOH, DCM, rt, 90%; (c) (i) Bu₂SnO, toluene, 105 °C; (ii) **18**, CsF, toluene, 105 °C, ∼20% (**19**), ∼20% (**20**) (Table S3†); (d) (i) Bu₂SnO, toluene, 105 °C; (ii) benzyl bromide, TBABr, toluene, 70 °C; (iii) Ac₂O, pyridine, rt, 91% over 2 steps; (e) Pd(OH)₂/C, H₂, EtOAc, rt, 86%; (f) **3**, TfOH, DCM, −40 °C to rt, ∼30% (Table S5†); (g) methyl benzoate, *hv* (254 nm), Et₂O/isopropanol, rt; (h) NaOMe, MeOH, rt, ∼30% over 2 steps (Table S6†).

bromide, which was subsequently activated with stoichiometric I₂ in the presence of isopropanol to obtain **17**, according to a method reported by Field and colleagues.[38] Deacetylation gave IPG (**15**) in 90% yield. Stannylene acetal-mediated alkylation of IPG (**15**) with (*Z*)-3-bromocyclooct-1-ene (**18**) in the presence of CsF or TBAI as an additive at 105 °C was initially investigated (Table S3†). A mixture of 3-CCO-IPG (**19**, ∼20% yield) and 6-CCO-IPG (**20**, ∼20% yield) was obtained and purified *via* (laborious) chromatographic separation. Decomposition of **18** at high temperature into 1,3-cyclooctadiene and hydrogen bromide[39] limited its use. Attempts to alkylate 6-TBS and 4,6-DTBS functionalized derivatives of **15** in a regioselective manner with **18** were unsuccessful (Table S4†).

Instead, IPG (**15**) was regioselectively benzylated using organotin chemistry followed by acetylation to obtain 2,4,6-OAc-3-OBn-IPG (**21**) in 91% yield over two steps. Hydrogenation of **21** in the presence of Pearlman's catalyst afforded 2,4,6-OAc-IPG (**22**) in 86% yield. Alkylation of **22** could be achieved in the timespan of hours at low temperature (≤0 °C), typically employing 4 equivalents of trichloroimidate **3** and 10 mol% of triflic acid (Table S5†). The crude reaction mixture was washed with aqueous NaOH (to remove **9**)[40] before purification by silica gel chromatography to obtain **23** in ≥30% yield. Singlet sensitized photoisomerization of **23** to **24** (Table S6†) was executed with the general flow setup described by Fox and co-workers[25] using silver(I) exchanged tosic acid silica gel (TAg silica) as the stationary phase.[41] Irradiation ($\lambda = 254$ nm) of mixture of **23** and methyl benzoate in Et₂O for ±24 h, whilst continuously circulating the reaction mixture over the stationary phase, was followed by treatment of the stationary phase with NH₃ in MeOH
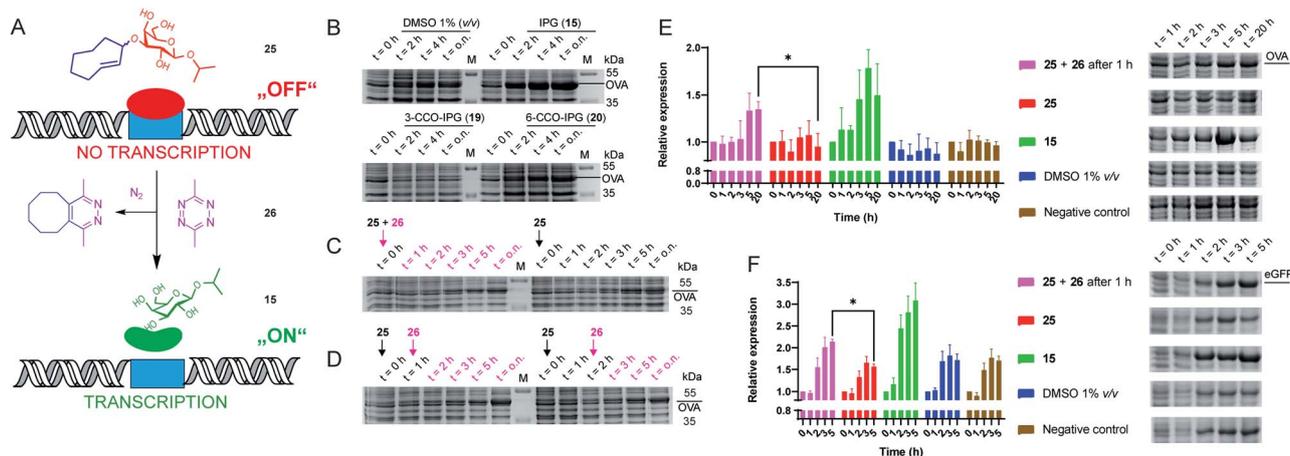

Scheme 3 Evaluation of the fate of peracetylated IPTG (**14**) during photoisomerization conditions. Reagents/conditions: (a) Ac₂O, pyridine, rt, 100%; (b) methyl benzoate, *hv* (254 nm), Et₂O, heptane, rt; (c) NH₄OAc (aq), DCM, rt, 61%.

Fig. 2 Recombinant expression of proteins with caged IPG variants. (A) Schematic representation of the chemical control over *lac* operon activity, mediated by 3-TCO-IPG (**25**), which does not induce expression. IEDDA pyridazine elimination with 3,6-dimethyl-tetrazine (**26**) liberates IPG (**15**), which induces overexpression of the protein of interest. (B) Recombinant OVA expression, comparing the effects of DMSO (negative control, 1% v/v), IPG (**15**, positive control, 1 mM), 3-CCO-IPG (**19**, 1 mM) and 6-CCO-IPG (**20**, 1 mM). The respective compounds were added at $t = 0$ h after which protein expression was followed over time. (C and D) Temporal control of OVA expression *via* addition of tetrazine **26** (2.5 mM) in the presence of 3-TCO-IPG (**25**, 1 mM). (C) Direct addition of **25** and **26** at $t = 0$ h (left) or addition of **25** at $t = 0$ h (right). (D) Addition of **26** 1 h (left) or 2 h (right) after adding **25** at $t = 0$ h. (E and F) Replicate expression experiments for OVA (2E; $N = 3$) and eGFP_A206K (2F; $N = 4$) comparing decaging conditions (1 mM **25** at $t = 0$ and 2.5 mM **26** at $1 = 1$ h) with addition of **25** (1 mM), **15** (1 mM), DMSO (1% v/v) and a negative control. Mean quantification values (Coomassie) were plotted with SD as error bars. Representative gel sections are shown to serve as an example. Full gels for all replicate experiments are shown in the ESI (Fig. S6–S12†). Relative band intensity was measured *via* densitometry for all experiments. For eGFP (2F), quantification was based on the Coomassie signal of the monomeric protein. *Significant difference based on an unpaired, two-tailed t-test ($P < 0.05$).

to obtain (partially deacetylated) **24**. Zemplén deacetylation of **24** afforded **25** after extractive desalting in ≥30% yield over 2 steps. This final product, 3-TCO-IPG (**25**), was exclusively obtained as the desired axial TCO isomer and its purity was optimized by carefully increasing the polarity of the photoisomerization reaction mixture with isopropanol (2–5%; Fig. S1†).

We next evaluated whether the TCO-modified IPG **25** could be used to control the function of the parent molecule (**15**) in a biological setting (Fig. 2A). For this we transformed *E. coli* to express the model protein ovalbumin (OVA) under control of the *lac* operon. Overnight cultures were inoculated in LB medium supplemented with 1% glucose to inhibit leaky expression. Next, cultures were grown in fresh LB medium (no glucose) before adding (caged) inducers (1 mM) and tetrazine (2.5 mM) in DMSO. We first tested whether IPG (**15**) could induce expression, which it did in a comparable level to IPTG (**13**; Fig. 2B, S2 and Table S7†). Furthermore, up to 10% DMSO was tolerated for IPG (**15**) induced OVA expression (Fig. S3 and Table S8†).

To assess the functionality of the TCO-protecting group, we confirmed 3-TCO-IPG (**25**) did not affect expression levels in absence of a deprotection agent (Fig. S4 and Table S9†). Subsequently, we analyzed whether deprotection with the prokaryote-compatible 3,6-dimethyl-tetrazine (**26**) could be used to switch on recombinant protein expression.[12,42] We found that **26** caused a minor delay on IPG (**15**) induced OVA expression without reducing overall expression levels (Fig. S5 and Table S10†).

Therefore, deprotection of 3-TCO-IPG (**25**) with **26** was studied in a time course experiment (Fig. 2C and D). Simultaneous addition of both **25** and **26** at the same time did not result in a controlled overexpression. However, a preincubation of 1 or 2 hours with **25** before addition of **26** did result in tightly controlled overexpression of OVA. This was particularly striking at late time points (Fig. 2D and Table S11†). Replicate experiments ($N = 3$) confirmed these findings (Fig. 2E, S6–S8 and Tables S12–S15†). Control compounds 3-CCO-IPG (**19**) and 6-CCO-IPG (**20**) failed to induce overexpression (Fig. 2B and Table S16†). A reduction in expression compared to the DMSO background was even observed for **19** (Fig. S4 and Table S9†), but this was not a property of the CCO-moiety in general.

The method was next applied to the expression of two other proteins, eGFP (Fig. 2F, S9–S12 and Tables S17–S21;† $N = 4$) and DsRed2 (Fig. S13†). Again, overexpression after addition of **26** was observed for both proteins based on Coomassie quantification (Fig. 2F and Table S22†). For eGFP, a significant overexpression was found after 5 hours (Fig. 2F). Taken together, it appears this chemical method can be utilized as a general tool for temporally controlled gene expression in *E. coli*.

Conclusions

In conclusion, we report the synthesis of TCO-ethers using two novel reagents (**2–3**), providing facile access to TCO-protected phenols and aliphatic alcohols, respectively. This methodology enables access to the modification of complex biomolecules as TCO-ethers. A carbohydrate probe, 3-TCO-IPG (**25**),

made in this manner was successfully used to chemically modulate *lac* operon activity, thereby providing a first example of control over glycan activity by IEDDA pyridazine elimination. The spatiotemporal control available to this method also bodes well for other applications in which carbohydrate/receptor interactions direct biological processes.

Conflicts of interest

There are no conflicts to declare.

Acknowledgements

Notes and references

1 J. Li and P. R. Chen, *Nat. Chem. Biol.*, 2016, **12**, 129–137.
2 J. Tu, M. Xu and R. M. Franzini, *ChemBioChem*, 2019, **20**, 1615–1627.
3 K. Neumann, A. Gambardella and M. Bradley, *ChemBioChem*, 2019, **20**, 872–876.
4 N. K. Devaraj, *ACS Cent. Sci.*, 2018, **4**, 952–959.
5 R. M. Versteegen, R. Rossin, W. ten Hoeve, H. M. Janssen and M. S. Robillard, *Angew. Chem., Int. Ed.*, 2013, **52**, 14112–14116.
6 M. L. Blackman, M. Royzen and J. M. Fox, *J. Am. Chem. Soc.*, 2008, **130**, 13518–13519.
7 J. C. T. Carlson, H. Mikula and R. Weissleder, *J. Am. Chem. Soc.*, 2018, **140**, 3603–3612.
8 R. M. Versteegen, W. ten Hoeve, R. Rossin, M. A. R. de Geus, H. M. Janssen and M. S. Robillard, *Angew. Chem., Int. Ed.*, 2018, **57**, 10494–10499.
9 B. L. Oliveira, Z. Guo and G. J. L. Bernardes, *Chem. Soc. Rev.*, 2017, **46**, 4895–4950.
10 J. Li, S. Jia and P. R. Chen, *Nat. Chem. Biol.*, 2014, **10**, 1003–1005.
11 G. Zhang, J. Li, R. Xie, X. Fan, Y. Liu, S. Zheng, Y. Ge and P. R. Chen, *ACS Cent. Sci.*, 2016, **2**, 325–331.
12 J. Zhao, Y. Liu, F. Lin, W. Wang, S. Yang, Y. Ge and P. R. Chen, *ACS Cent. Sci.*, 2019, **5**, 145–152.
13 R. Rossin, R. M. Versteegen, J. Wu, A. Khasanov, H. J. Wessels, E. J. Steenbergen, W. ten Hoeve, H. M. Janssen, A. H. A. M. van Onzen, P. J. Hudson and M. S. Robillard, *Nat. Commun.*, 2018, **9**, 1484.
14 R. Rossin, S. M. J. van Duijnhoven, W. ten Hoeve, H. M. Janssen, F. J. M. Hoeben, R. M. Versteegen and M. S. Robillard, *Bioconjugate Chem.*, 2016, **27**, 1697–1706.
15 S. Du, D. Wang, J.-S. Lee, B. Peng, J. Ge and S. Q. Yao, *Chem. Commun.*, 2017, **53**, 8443–8446.

16 I. Khan, L. M. Seebald, N. M. Robertson, M. V. Yigit and M. Royzen, *Chem. Sci.*, 2017, **8**, 5705–5712.
17 Q. Yao, F. Lin, X. Fan, Y. Wang, Y. Liu, Z. Liu, X. Jiang, P. R. Chen and Y. Gao, *Nat. Commun.*, 2018, **9**, 5032.
18 J. M. Mejia Oneto, I. Khan, L. Seebald and M. Royzen, *ACS Cent. Sci.*, 2016, **2**, 476–482.
19 M. Czuban, S. Srinivasan, N. A. Yee, E. Agustin, A. Koliszak, E. Miller, I. Khan, I. Quinones, H. Noory, C. Motola, R. Volkmer, M. Di Luca, A. Trampuz, M. Royzen and J. M. Mejia Oneto, *ACS Cent. Sci.*, 2018, **4**, 1624–1632.
20 S. Davies, L. Qiao, B. L. Oliveira, C. D. Navo, G. Jiménez-Osés and G. J. L. Bernardes, *ChemBioChem*, 2019, **20**, 1541–1546.
21 S. Davies, B. L. Oliveira and G. J. L. Bernardes, *Org. Biomol. Chem.*, 2019, **17**, 5725–5730.
22 E. Jiménez-Moreno, Z. Guo, B. L. Oliveira, I. S. Albuquerque, A. Kitowski, A. Guerreiro, O. Boutureira, T. Rodrigues, G. Jiménez-Osés and G. J. L. Bernardes, *Angew. Chem., Int. Ed.*, 2017, **56**, 243–247.
23 K. Neumann, S. Jain, A. Gambardella, S. E. Walker, E. Valero, A. Lilienkampf and M. Bradley, *ChemBioChem*, 2017, **18**, 91–95.
24 H. Wu, S. C. Alexander, S. Jin and N. K. Devaraj, *J. Am. Chem. Soc.*, 2016, **138**, 11429–11432.
25 M. Royzen, G. P. A. Yap and J. M. Fox, *J. Am. Chem. Soc.*, 2008, **130**, 3760–3761.
26 S. Fletcher, *Org. Chem. Front.*, 2015, **2**, 739–752.
27 F. Guibe and Y. S. M'leux, *Tetrahedron Lett.*, 1981, **22**, 3591–3594.
28 J. Muzart, *Tetrahedron*, 2005, **61**, 5955–6008.
29 A. R. Haight, E. J. Stoner, M. J. Peterson and V. K. Grover, *J. Org. Chem.*, 2003, **68**, 8092–8096.
30 F. Cramer and N. Hennrich, *Chem. Ber.*, 1961, **94**, 976–989.
31 H.-P. Wessel, T. Iversen and D. R. Bundle, *J. Chem. Soc., Perkin Trans. 1*, 1985, 2247.
32 F. Jacob and J. Monod, *J. Mol. Biol.*, 1961, **3**, 318–356.
33 M. Lewis, *C. R. Biol.*, 2005, **328**, 521–548.
34 C. E. Bell and M. Lewis, *Nat. Struct. Biol.*, 2000, **7**, 209–214.
35 M. Lewis, *J. Mol. Biol.*, 2013, **425**, 2309–2316.
36 D. D. Young and A. Deiters, *Angew. Chem., Int. Ed.*, 2007, **46**, 4290–4292.
37 S. L. Collins, J. Saha, L. C. Bouchez, E. M. Hammond and S. J. Conway, *ACS Chem. Biol.*, 2018, **13**, 3354–3360.
38 K. P. R. Kartha, M. Aloui and R. A. Field, *Tetrahedron Lett.*, 1996, **37**, 8807–8810.
39 S. Kobayashi, K. Fukuda, M. Kataoka and M. Tanaka, *Macromolecules*, 2016, **49**, 2493–2501.
40 M. Heuckendorff and H. H. Jensen, *Carbohydr. Res.*, 2017, **439**, 50–56.
41 A. Darko, S. J. Boyd and J. M. Fox, *Synthesis*, 2018, **50**, 4875–4882.
42 L. Liu, Y. Liu, G. Zhang, Y. Ge, X. Fan, F. Lin, J. Wang, H. Zheng, X. Xie, X. Zeng and P. R. Chen, *Biochemistry*, 2018, **57**, 446–450.